

Surface modification on polydimethylsiloxane-based microchannels with fragmented poly(L-lactic acid) nanosheets

Lu Yang,¹ Yosuke Okamura,^{1,2} and Hiroshi Kimura^{1,3}

¹*Micro/Nano Technology Center, Tokai University, 4-1-1 Kitakaname, Hiratsuka, Kanagawa 259-1292, Japan*

²*Department of Applied Chemistry, Tokai University, 4-1-1 Kitakaname, Hiratsuka, Kanagawa 259-1292, Japan*

³*Department of Mechanical Engineering, Tokai University, 4-1-1 Kitakaname, Hiratsuka, Kanagawa 259-1292, Japan*

(Received 4 October 2015; accepted 11 November 2015; published online 20 November 2015)

Surface modification is a critical issue in various applications of polydimethylsiloxane (PDMS)-based microfluidic devices. Here, we describe a novel method through which PDMS-based microchannels were successfully modified with fragmented poly(L-lactic acid) (PLLA) nanosheets through a simple patchwork technique that exploited the high level of adhesiveness of PLLA nanosheets. Compared with other surface modification methods, our method required neither complicated chemical modifications nor the use of organic solvents that tend to cause PDMS swelling. The experimental results indicated that the modified PDMS exhibited excellent capacity for preventing the adhesion and activation of platelets. This simple yet efficient method can be used to fabricate the special PDMS microfluidic devices for biological, medical, and even hematological purposes. © 2015 AIP Publishing LLC.

[<http://dx.doi.org/10.1063/1.4936350>]

I. INTRODUCTION

In recent years, microfluidic devices have attracted much attention for their widespread applications in chemical analysis, material preparation, and biomedical fields owing to their competitive advantages, such as minimal reagent consumption, excellent controllability, and superior integratability.^{1–3} In the fabrication of microfluidic devices, polydimethylsiloxane (PDMS) is the most popular material; this can be attributed to its remarkable features, including optical transparency, relatively high chemical inertness, low manufacturing cost, and ease of molding.^{4–6} However, the hydrophobic PDMS surface makes it difficult to fill the microchannel with aqueous solutions, and adsorption of organic analytes, resulting in nonspecific adsorption of biomolecules, is likely to occur. These disadvantages have somewhat limited the use of PDMS-based microfluidic devices. Therefore, appropriate modification of PDMS surfaces is necessary in order to adapt these materials to various demands, especially in the field of biomicrofluidics.

Many methods for surface modification have been developed to enhance the applicability of PDMS-based microfluidic devices. These methods have been broadly classified into two categories: physical methods and chemical methods, depending on whether there is a chemical change.^{7,8} Typical examples of physical methods include chemical vapor deposition (CVD), particle coating, and adsorption of amphiphilic molecules.⁹ The most commonly used method is dynamic modification with surfactants or proteins whose hydrophobic tails are easily adsorbed onto the PDMS surface. Although such modifications can change the surface properties of the PDMS *in situ*, the molecules can undergo desorption caused by their weak bonding with native PDMS, leading to short-term applicability. Examples of these types of chemical modifications include plasma treatment, UV treatment, silanization, and graft polymerization.¹⁰ Exposure of the PDMS surface to oxygen plasma will result in oxidation and increased hydrophilicity.

However, the low glass transition temperature of PDMS makes the hydrophobic recovery unavoidable and rapid (i.e., within 4 days).¹¹ Some efforts have been made to minimize this hydrophobic recovery, such as the optimization of curing conditions and vacuum treatment time prior to plasma treatment,¹² whereas it is still not a permanent modification. Plasma-based treatment allows the PDMS surface to generate silanol groups that can react with polymers, thereby introducing a specific chemical functionality into the surface. Additionally, many post-bonding modification methods including photolithography and electrochemical bio-lithography have been developed to add some more sensitive functionalities.¹³ Nevertheless, these methods are always accompanied by complicated procedures and the use of organic solvents that may cause swelling of the PDMS. Therefore, developing a simpler and more reliable surface modification method for fabricating PDMS-based microfluidic devices remains a challenge.

Besides these methods mentioned above, Sibarani *et al.*¹⁴ also presented a simple method for coating the PDMS surface with biocompatible polymers using only a solvent evaporation procedure. Notably, the coated surface decreased protein adsorption because the structures of phosphorylcholine groups within these polymers were similar to the structure of the cell membrane. Additionally, poly(L-lactic acid) (PLLA), another important biocompatible and biodegradable polymer, has been fabricated as an ultrathin film (often referred to as a nanosheet) for application as a sealing material in surgery.¹⁵ This freestanding nanosheet, which has a thickness of less than 100 nm, has been shown to have high potential to adhere to glass, plastic, skin, and organs without the use of adhesive reagents. Furthermore, fragmented nanosheets, which refers to the fragments of nanosheet fabricated by homogenization of the original nanosheet, can also be used to coat both broad and irregular surfaces.¹⁶

These unique studies inspired us to attempt to use fragmented PLLA nanosheets to coat PDMS-based microchannels, which have been attracting attention for their potential applications as human blood vessel mimics in the hematological field.^{17–20} Accordingly, some typical modification methods have been reported as a useful way to increase the blood compatibility of PDMS microchannels, such as polyethylene glycol (PEG) graft,^{21,22} heparin,²³ and betaine polymers coating.²⁴ In this paper, we developed a novel method for modifying PDMS and examined the surface properties of the modified PDMS, particularly the capacity for platelet adhesion. Our method of physical modification was more independent of the changes in the PDMS polymer structure than traditional chemical modifications and can thus prevent the hydrophobic recovery of the surface layer. This work provided important new insights on PDMS surface modification.

II. MATERIALS AND METHODS

In our experiments, the surface characterization including contact angle measurement, X-ray photoelectron spectroscopy (XPS) analysis, and evaluation of platelet adhesion to sample surfaces for nanosheet-coated PDMS plates was first carried out. Meanwhile, the coating process for PDMS microchannels as well as platelet adhesion to channel walls under flow conditions were investigated. These procedures are described in detail in this section.

A. Microfluidic device

A common straight microchannel was designed as a simple model of the microvasculature. The dimensions of the microchannel were $500\ \mu\text{m}$ (height) \times $500\ \mu\text{m}$ (width) \times $45\ \text{mm}$ (length). To fabricate the PDMS-based microfluidic device, a mold was made from a SU-8 2100 resist (MicroChem Corp., MA, USA) on a silicon wafer by conventional photolithography.^{25–27} A mixture of uncured PDMS and curing agent (10:1 w/w) was thoroughly mixed and poured into the mold, followed by degassing and heating at 75°C for 3 h. Next, the PDMS replica was peeled off, punched to provide an inlet and outlet, and then sealed with another PDMS sheet using a plasma cleaner (Expanded Plasma Cleaner PDC-32G; Harrick Plasma, NY, USA). The outlet was connected to a syringe pump (Microfluidic System Works Inc., Tokyo, Japan) through a silicone tube.

B. Coating method

Aqueous suspensions of fragmented PLLA (Mw: 80–100 kDa; Polysciences Inc., PA, USA) nanosheets were prepared using a multilayered spin-coating and homogenization process described in our previous work.¹⁶ DIO-conjugated (DIOC₁₈; Molecular Probes, Inc., OR, USA) fragmented PLLA nanosheets were also made for fluorescence microscopy. The mean area and thickness of the prepared nanosheet fragments were $7400\ \mu\text{m}^2$ and $60 \pm 6\ \text{nm}$, respectively. A unique property of the PLLA nanosheet allowed the nanosheets to adhere firmly to the PDMS surface upon water evaporation. PDMS plates made of cured PDMS with dimensions of 1 mm (thickness) \times 10 mm (width) \times 10 mm (length) were prepared prior to the coating procedure. In the case of the plate coating, the nanosheet suspension was dripped on the plate at the required volume and was then placed in a drying closet overnight. For microchannel coating, a nanosheet suspension of $20\ \mu\text{l}$ was added to the inlet reservoir and passed through the channel by pulling a syringe at the outlet. The microchannel filled with the nanosheet suspension was heated in an oven at 90°C for 30 min to facilitate water evaporation, leading to the firm binding of nanosheets to the channel wall. These perfusion and drying steps constituting a coating procedure cycle were repeated several times until the inner surface of the microchannel was covered completely. ImageJ software was used to manually analyze the coverage ratio of nanosheets, which was determined by measuring the percentage of the area covered by fragmented nanosheets relative to the entire area of the microchannel. The modified microchannel was then washed with phosphate-buffered saline (PBS) pumped at high flow rates of 1 and 2 ml/min to test its long-term durability.

C. Characterization of the modified surface

The water contact angles of native and nanosheet-coated PDMS surfaces were measured on three different locations for each sample. XPS (ULVAC-PHI Inc., Kanagawa Japan) was carried out to determine the chemical composition of the surface layer (C1s, O1s, and Si2p). The take-off angle of the photoelectron was 45° , and analysis areas were $100\ \mu\text{m} \times 100\ \mu\text{m}$ for the survey scan and $50\ \mu\text{m} \times 50\ \mu\text{m}$ for the narrow scan.

Platelet adhesion to the PDMS surface was also evaluated. Human blood samples were obtained from healthy donors by trained professionals following procedures that complied with relevant ethical regulations. Platelet rich plasma (PRP) was prepared by centrifugation of the blood samples at $120 \times g$ for 15 min using 0.38 vol. % sodium citrate as the anticoagulant.

Three categories of samples consisting of native (negative control), bovine serum albumin (BSA)-coated, and nanosheet-coated PDMS plates were kept in 24-well plates. To prepare BSA-coated PDMS plates, here, the native PDMS plates were pretreated with BSA (Sigma-Aldrich, MO, USA) by immersing them in 30 mg/ml BSA-PBS solution for 2 h. Next, $350\ \mu\text{l}$ PRP was added into each well, and the 24-well plates were then placed in an incubator at 37°C for 0.5, 1, 2, or 3 h. The PDMS plates were then washed with PBS solution at least three times to remove unbound platelets, followed by fixation of the adherent platelets using 2.5% glutaraldehyde. A fluorescent dye (FM 1–43; 5 mM; Molecular Probes, Inc., OR, USA) was used to label the platelet membrane for microscopic observation. Quantitative analysis of fluorescent images was carried out using ImageJ. The ratio of the area covered by the platelets to the full field of view was calculated by determining the numbers of pixels. Because PLLA nanosheets were slightly stained by FM 1–43 as well, the images were manually and carefully analyzed to eliminate the effects of background before measurement. Moreover, PRP-treated PDMS plates were freeze dried and sputter-coated with gold (SANYU ELECTRON, SC-701) at an ion current of 3 mA for 1 min. Scanning electron microscopy (SEM; S-4800; Hitachi High-Technologies Corp., Tokyo, Japan) was then carried out at an accelerating voltage of 3 keV.

For the platelet adhesion assessment under flow condition, PRP was perfused into the native and modified microchannels incubated in 37°C water bath at a flow rate of $200\ \mu\text{l}/\text{min}$ for 30 min. The analysis method was the same as that for PDMS plate assessment.

III. RESULTS AND DISCUSSION

A. Characterization of the modified surfaces

The PDMS plates were coated with fragmented nanosheets by dripping the nanosheet suspension on the plate and drying it with air. This physical modification was more independent of the changes in the PDMS polymer structure than traditional chemical modifications and can thus prevent the hydrophobic recovery of the surface layer. The morphology of the modified surfaces is shown in Figure 1. The patchwork of fragmented nanosheets exhibited some wrinkles and ridges due to the flexibility of the ultrathin PLLA nanosheets and their overlap. However, they did not affect the optical transparency of PDMS, particularly with solution perfusion.

The modified surfaces were characterized with water contact angle measurements. The contact angle decreased from 112.9° for the native PDMS surface to 81.0° for the PLLA nanosheet-coated PDMS surface. This result could be explained by the replacement of the siloxane chain of PDMS with the ester groups of PLLA by simply coating the PDMS surface with the PLLA fragmented nanosheets.

Additionally, XPS analysis was performed to examine the elemental components of the sample surfaces. As shown in Figure 2, the atomic compositions of the surface layer showed that only extremely trace amounts of silicon could be detected in the nanosheet-coated surface in comparison with the native PDMS surface. This detection of silicon may be caused by the influence of the PDMS substrate, which was partially exposed to X-rays owing to small gaps in the nanosheet patchwork. However, since there were just a few gaps, their negative effects were considered negligible. In future studies, it will be necessary to further decrease the take-off angle of the photoelectron in order to eliminate the effects of the substrate. Moreover, there was a clear difference in the C1s signal peak between the two samples. In the case of the PLLA nanosheet-coated sample, the C1s peak was split into three subpeaks, representing the C-H signal of the methyl group at 284.0 eV, the C-O signal at 285.9 eV, and the C=O signal of the carboxylic group at 288.4 eV. These subpeaks were consistent with the characteristic molecular structures of PLLA,^{15,29} supporting the presence of PLLA in the surface layer. From these results, we concluded that the modified PDMS surface was almost completely covered by the fragmented PLLA nanosheets.

In addition, for some studies involving establishment of mimetic blood vessel models, microchannels are required to prevent platelet adhesion, similar to human vessel walls. However, due to the low blood compatibility of the PDMS surface, a blocking agent (e.g., BSA) has generally been used to coat the PDMS and inhibit cell adsorption.^{17,18,30} Accordingly, we next examined the extent of platelet adhesion to native PDMS surfaces, BSA-coated PDMS surfaces, and nanosheet-coated PDMS surfaces in order to validate the applicability of modified PDMS devices for hematological use. Various PDMS plates immersed in PRP were incubated for different hours before the observation. As shown in Figure 3(a), for the native PDMS plates, there was a large area of the surface that was covered by adherent platelets, indicating that this

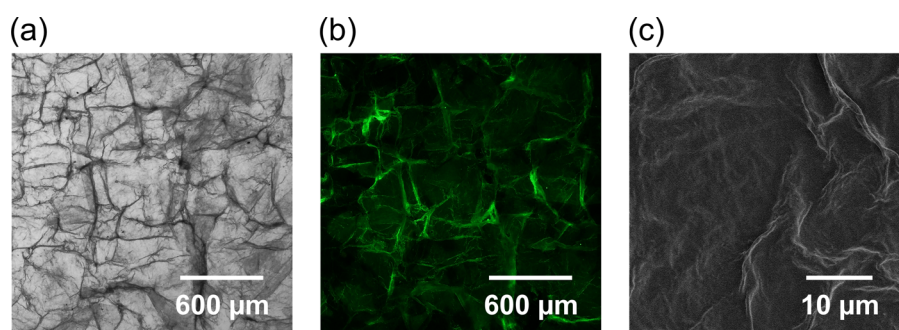


FIG. 1. Typical images showing the morphology of the PLLA nanosheet-coated PDMS surfaces. (a) Bright-field image. (b) Fluorescent image of the surface coated with DIO-conjugated PLLA nanosheet. (c) SEM image.

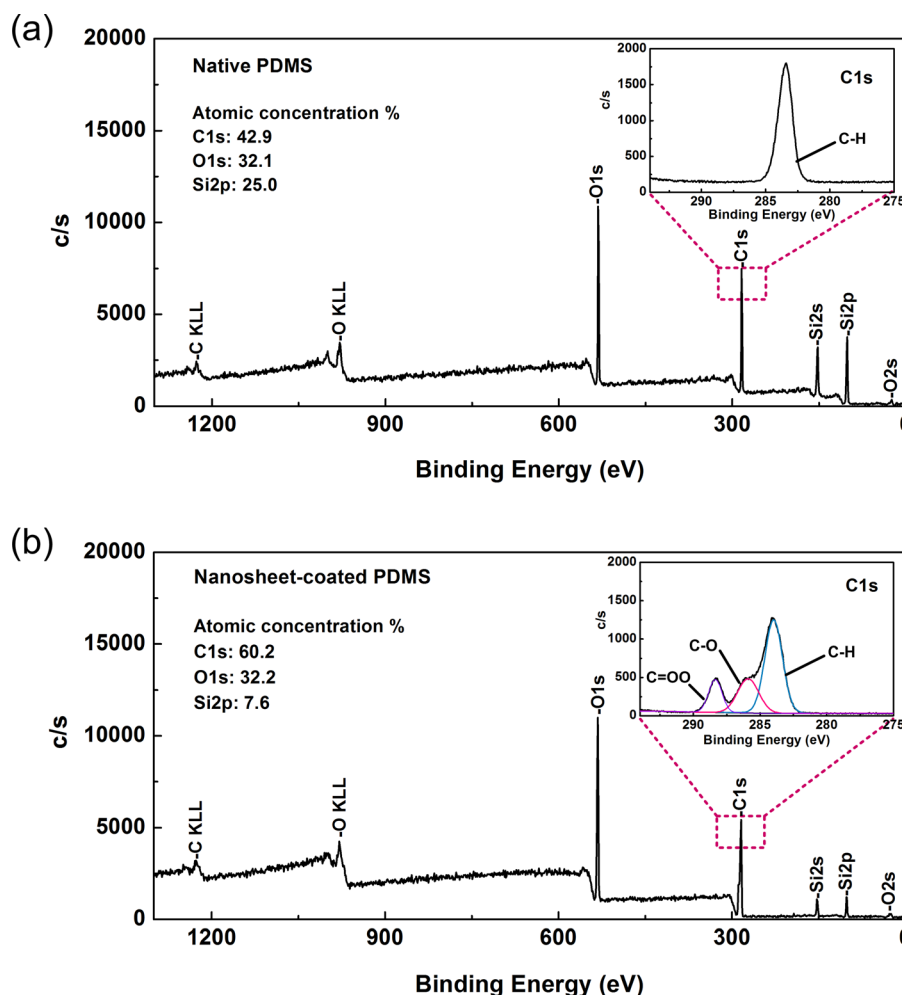


FIG. 2. XPS analysis of (a) native and (b) PLLA nanosheet-coated PDMS surfaces. The inset shows the details of the narrow scan for the C1s signal. The step sizes for the survey scan and narrow scan were 1 and 0.05 eV, respectively.

material facilitated capture of platelets. In contrast, for the nanosheet-coated PDMS plates, only a few platelets were found to have attached to the surface, suggesting that the coating procedure should prevent platelet adhesion, even during long-term exposure to PRP for up to 3 h. As our control, we found that the BSA-coated PDMS plates exhibited clear suppression of platelet adhesion; however, this effect was not sufficient for practical utilization. Therefore, our method provided a more efficient way to avoid platelet adhesion to the PDMS surface.

Platelet adhesion is known as a complex process induced by the interactions between the receptor on the platelet membrane and plasma proteins.^{31–33} Surface properties, such as functional group structure, wettability, charge, and topography, will significantly affect this adhesion process.^{28,34} Here, the resistance of platelet adhesion may be attributed to the inherent biocompatibility of PLLA and the unique microscale patterns of the fragmented nanosheet. However, the thorough exploration of this mechanism is beyond the scope of our current study and will be implemented in our future work.

We also found that the adherent platelets on the native PDMS surface spread and even aggregated forming a thrombus (Figure 3(b)). This result revealed that following adhesion, platelets experienced activation, and aggregation as a result of a series of complex responses induced by high-affinity binding between protein ligands and their receptors.^{35,36} Conversely, a trace amount of the adherent platelets on the nanosheet-coated PDMS surface remained in the

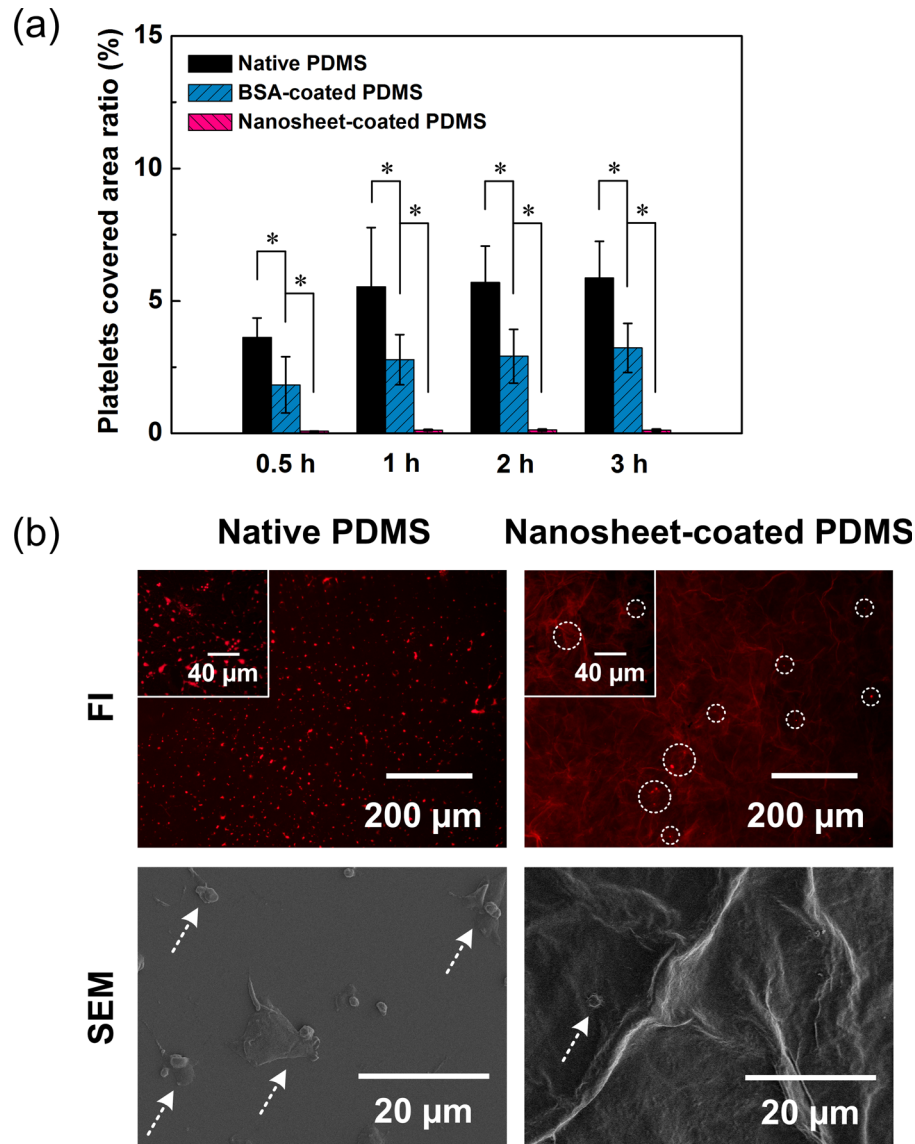


FIG. 3. (a) Adherent platelets on various sample surfaces. The horizontal axis represents the incubation time, and the vertical axis is the ratio of the area covered by platelets to the full field of view. Data are the means \pm SDs ($n = 6$). *: $p < 0.05$ using t tests for the indicated comparisons. (b) Typical fluorescent images (FIs) and SEM images of native and nanosheet-coated PDMS with platelet adhesion. A fluorescent dye FM 1-43 was used to label the platelet membrane for fluorescence microscopy. The circles in FI and arrows in SEM images mark the position of adherent platelets.

resting status without activation. Thus, the modified PDMS surface could inhibit both platelet adhesion and activation.

B. Microchannel coating

Next, we determined the experimental conditions necessary for microchannel coating. In our experiments, PDMS microchannels were filled with the nanosheet suspension and then dried in an oven for coating them with fragmented nanosheets. These perfusion and drying steps constituted a coating cycle. The coating cycle number and the concentration of the nanosheet suspension were considered the two main factors for optimization. As shown in Figure 4(a), the nanosheet coverage ratio increased gradually with the increase in coating cycle number. Moreover, as expected, fewer coating cycles were required to coat the channel inner surface

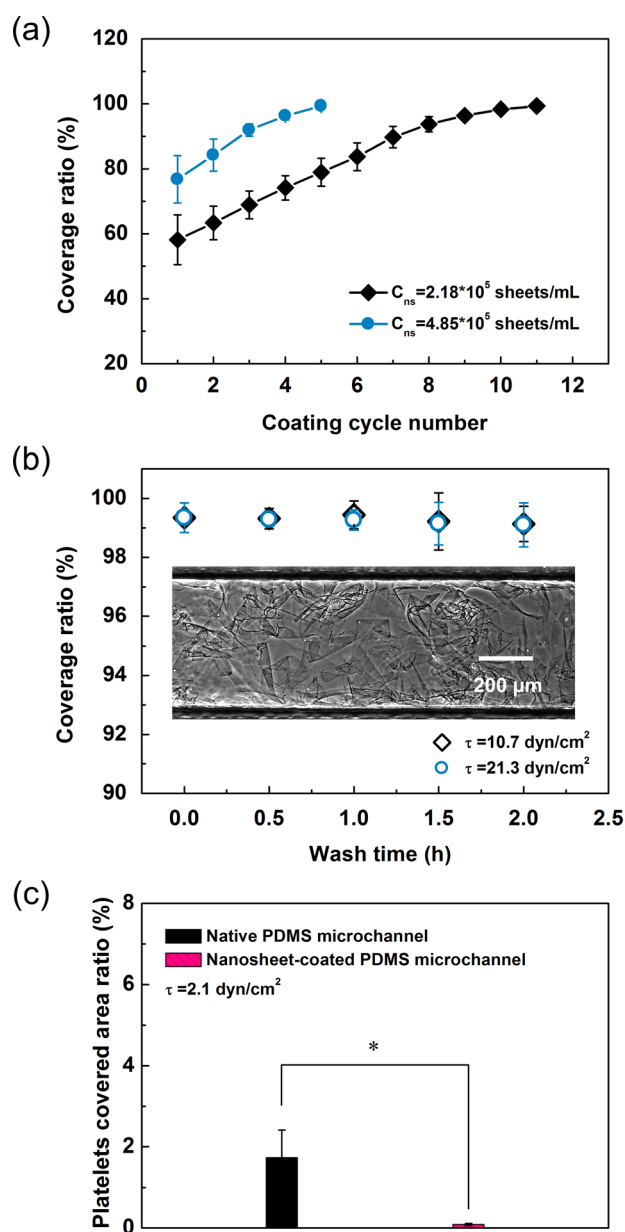


FIG. 4. (a) Evolution of the coverage ratio according to different coating times. Data are the means \pm SDs ($n=8$). (b) Long-term durability of the modified microchannels under strong fluid shear stress. The inset is a typical image of a microchannel inner surface coated with fragmented nanosheets captured in phase-contrast mode. Data are the means \pm SDs ($n=5$). (c) Platelet adhesion assessment under flow condition. Data are given as means \pm SDs ($n=7$). *: $p < 0.005$ using t tests for the indicated comparisons.

completely when using nanosheet suspensions with higher concentrations. Nevertheless, fragmented nanosheets clogged the microchannel inlet when the suspension concentration exceeded 6.0×10^5 sheets/mL. These results revealed that the most efficient method for achieving a high coverage ratio was to repeat the coating procedure several times and use a nanosheet suspension with a relatively higher concentration.

In a previous study, we described the extremely good adhesion strength of the PLLA nanosheet using a static microscratch method.¹⁵ In this study, we examined the long-term durability of the nanosheet-coated microchannel under dynamic flow conditions. As shown in Figure 4(b), the coverage ratio remained nearly unchanged, even after undergoing quite high shear stresses

of 10.7 dyn/cm² and 21.3 dyn/cm² for an extended duration. This result demonstrated that the PLLA nanosheet was difficult to detach once it had dried on the PDMS surface. Human blood shear stress usually ranges from 0.8 to 8 dyn/cm² for venous circulation and from 10 to 60 dyn/cm² for arterial circulation;¹⁷ therefore, our modified microchannel could resist *in vitro* mimetic blood flow conditions with long-term availability. Additionally, PRP was perfused into the microchannels with a shear stress of 2.1 dyn/cm². Notably, as shown in Figure 4(c), the results of platelet adhesion assessment were similar to those of the PDMS plate.

IV. CONCLUSION

In this study, a novel method was developed to modify the PDMS surface in order to achieve more widespread utilization of PDMS-based microfluidic devices. We found that platelet adhesion and activation were prevented under both the static and flow conditions. Moreover, investigation of the necessary experimental conditions for microchannel coating demonstrated the long-term durability of the modified microchannel. Our method was simple yet efficient and did not cause any damage to the PDMS-based microchannels. However, in order to coat microchannels with monolayer nanosheets, we may need to develop other *in situ* coating methods. Although we only used PLLA nanosheets in this study, the proposed method could be applicable to other fragmented nanosheets fabricated from polystyrene, polyimide, and other polymers to add different functionalities to the surfaces. The applications of this surface modification method, such as fabrication of microchips for antithrombotic drug tests, will be evaluated in our future studies.

ACKNOWLEDGMENTS

This study was supported by a grant of Strategic Research Foundation Grant-aided Project for Private Universities from Ministry of Education, Culture, Sport, Science, and Technology, Japan (MEXT).

- ¹L. Shui, J. C. T. Eijkel, and A. van den Berg, *Adv. Colloid Interface Sci.* **133**, 35–49 (2007).
- ²D. Dendukuri and P. S. Doyle, *Adv. Mater.* **21**, 4071–4086 (2009).
- ³L. Y. Yeo, H.-C. Chang, P. P. Y. Chan, and J. R. Friend, *Small* **7**, 12–48 (2011).
- ⁴J. C. McDonald, D. C. Duffy, J. R. Anderson, D. T. Chiu, H. K. Wu, O. J. A. Schueller, and G. M. Whitesides, *Electrophoresis* **21**, 27–40 (2000).
- ⁵J. C. McDonald and G. M. Whitesides, *Acc. Chem. Res.* **35**, 491–499 (2002).
- ⁶P. N. Nge, C. I. Rogers, and A. T. Woolley, *Chem. Rev.* **113**, 2550–2583 (2013).
- ⁷H. Makamba, J. Kim, K. Lim, N. Park, and J. Hahn, *Electrophoresis* **24**, 3607–3619 (2003).
- ⁸J. Zhou, A. Ellis, and N. Voelcker, *Electrophoresis* **31**, 2–16 (2010).
- ⁹J. Zhou, D. A. Khodakov, A. V. Ellis, and N. H. Voelcker, *Electrophoresis* **33**, 89–104 (2012).
- ¹⁰I. Wong and C.-M. Ho, *Microfluid. Nanofluid.* **7**, 291–306 (2009).
- ¹¹S.-K. Chae, C.-H. Lee, S. H. Lee, T.-S. Kim, and J. Y. Kang, *Lab Chip* **9**, 1957–1961 (2009).
- ¹²N. Lien, M. Hang, W. Wang, Y. Tian, L. Wang, T. J. McCarthy, and W. Chen, *ACS Appl. Mater. Interfaces* **6**, 22876–22883 (2014).
- ¹³C. Priest, *Biomicrofluidics* **4**, 032206 (2010).
- ¹⁴J. Sibarani, M. Takai, and K. Ishihara, *Colloids Surf., B* **54**, 88–93 (2007).
- ¹⁵Y. Okamura, K. Kabata, M. Kinoshita, D. Saitoh, and S. Takeoka, *Adv. Mater.* **21**, 4388–4392 (2009).
- ¹⁶Y. Okamura, K. Kabata, M. Kinoshita, H. Miyazaki, A. Saito, T. Fujie, S. Ohtsubo, D. Saitoh, and S. Takeoka, *Adv. Mater.* **25**, 545–551 (2013).
- ¹⁷E. Gutierrez, B. G. Petrich, S. J. Shattil, M. H. Ginsberg, A. Groisman, and A. Kasirer-Friede, *Lab Chip* **8**, 1486–1495 (2008).
- ¹⁸R. W. Muthard and S. L. Diamond, *Lab Chip* **13**, 1883–1891 (2013).
- ¹⁹X. Li, W. Chen, Z. Li, L. Li, H. Gu, and J. Fu, *Trends Biotechnol.* **32**, 586–594 (2014).
- ²⁰D. Kim, S. Finkenshaedt-Quinn, K. R. Hurley, J. T. Buchman, and C. L. Haynes, *Analyst* **139**, 906–913 (2014).
- ²¹S. Lee and J. Voros, *Langmuir* **21**, 11957–11962 (2005).
- ²²K. M. Kovach, J. R. Capadona, A. Sen Gupta, and J. A. Potkay, *J. Biomed. Mater. Res., Part A* **102**, 4195–4205 (2014).
- ²³S. Thorslund, J. Sanchez, R. Larsson, F. Nikolajeff, and J. Bergquist, *Colloids Surf., B* **45**, 76–81 (2005).
- ²⁴Z. Zhang, J. Borenstein, L. Guiney, R. Miller, S. Sukavaneshvar, and C. Loose, *Lab Chip* **13**, 1963–1968 (2013).
- ²⁵G. M. Whitesides, E. Ostuni, S. Takayama, X. Y. Jiang, and D. E. Ingber, *Annu. Rev. Biomed. Eng.* **3**, 335–373 (2001).
- ²⁶B. D. Gates, Q. B. Xu, M. Stewart, D. Ryan, C. G. Willson, and G. M. Whitesides, *Chem. Rev.* **105**, 1171–1196 (2005).
- ²⁷H. Kimura, T. Yamamoto, H. Sakai, Y. Sakai, and T. Fujii, *Lab Chip* **8**, 741–746 (2008).
- ²⁸M. Ni, W. H. Tong, D. Choudhury, N. A. A. Rahim, C. Iliescu, and H. Yu, *Int. J. Mol. Sci.* **10**, 5411–5441 (2009).
- ²⁹E. Kiss, I. Bertoti, and E. I. Vargha-Butler, *J. Colloid Interface Sci.* **245**, 91–98 (2002).
- ³⁰L. E. Corum, C. D. Eichinger, T. W. Hsiao, and V. Hlady, *Langmuir* **27**, 8316–8322 (2011).

- ³¹B. Furie and B. C. Furie, [N. Engl. J. Med.](#) **359**, 938–949 (2008).
- ³²D. Varga-Szabo, I. Pleines, and B. Nieswandt, [Arterioscler., Thromb., Vasc. Biol.](#) **28**, 403–412 (2008).
- ³³Z. M. Ruggeri and G. L. Mendolicchio, [Circ. Res.](#) **100**, 1673–1685 (2007).
- ³⁴N. Weber, A. Pesnell, D. Bolikal, J. Zeltinger, and J. Kohn, [Langmuir](#) **23**, 3298–3304 (2007).
- ³⁵J. R. Kapoor, [N. Engl. J. Med.](#) **358**, 1638 (2008).
- ³⁶Y. Yoshimoto, T. Hasebe, K. Takahashi, M. Amari, S. Nagashima, A. Kamijo, A. Hotta, K. Takahashi, and T. Suzuki, [Microsc. Res. Tech.](#) **76**, 342–349 (2013).